J. Condensed Matter Nucl. Sci. 13 (2014) 565–578

Research Article

Physics of Cold Fusion by TSC Theory

Akito Takahashi*,†

Technova Inc., 1-1 Uchisaiwaicho 1-chome, Chiyoda-ku, Tokyo 100-0011, Japan

Abstract

This paper explains the basic physics of cold fusion by the tetrahedral symmetric condensate (TSC) theory. Models of TSC formation conditions in condensed matter are first proposed. Secondly formulas for cold fusion rates per D(H)-cluster are explained with typical quantitative results. The 4D/TSC fusion and the 4H/TSC WS fusion describe the D (deuterium)-system and the H (protium)-system, respectively.
 ISSN 2227-3123

Keywords: D(H)-cluster, 4D fusion, 4H WS fusion, TSC theory

1. Introduction

The tetrahedral symmetric condensate (TSC) theory has been elaborated for 23 years beginning in April 1989 [1]. The basic concept (by intuition) is that the ordering/constraint conditions of particles (namely deuterons, protons and electrons) in condensed matter containing deuterium (D) and/or protium (H) should make unique heretofore unknown D(H)-cluster fusion reactions measurable, while the known fusion reactions in high temperature plasma are two-body reactions such as p–d, d–d, d–t, d–^{3}He and so on, which take place in random free particle motions. Here, D(H)-cluster includes two deuterons (or protons) systems as d–e–d (p–e–p) and d–e–e–d (p–e–e–p), as well as 3D(H), 4D(H), 6D(H) and so forth. Here e denotes electron. D denotes deuteron (d) + electron (e), and H denotes p + e.

The study of D(H)-cluster dynamics using the quantum mechanical (QM) Langevin equation [2] shows that any transient entity (condensate state) as small as a few tens of femtometers will not be possible for the d–e–d and d–e–e–d systems or a 3D-cluster. On the other hand, a 4D/TSC- or a 6D/OSC-neutral-clusters may ultimately condense to a very small charge-neutral entity, as small as a few tens of femtometer or less. In this state, it will induce significant reaction rates of nuclear strong interaction between deuterons. The condensation time for 4D/TSC is as short as 1.4 fs and the yield of 4D/TSC fusion per TSC is 1.0 (100%) [3].

The macroscopic fusion rate by the TSC theory is given by the product of two rates as,

$$\langle \text{Macroscopic fusion rate} \rangle = \langle \text{D(H)} - \text{Cluster formation rate} \rangle \times \langle \text{Microscopic fusion yield per TSC} \rangle. \quad (1)$$

*E-mail: akito@sutv.zaq.ne.jp
†Also at: Osaka University, 1-1 Yamadaoka, Suita, Osaka 565-0871, Japan.

 ISSN 2227-3123

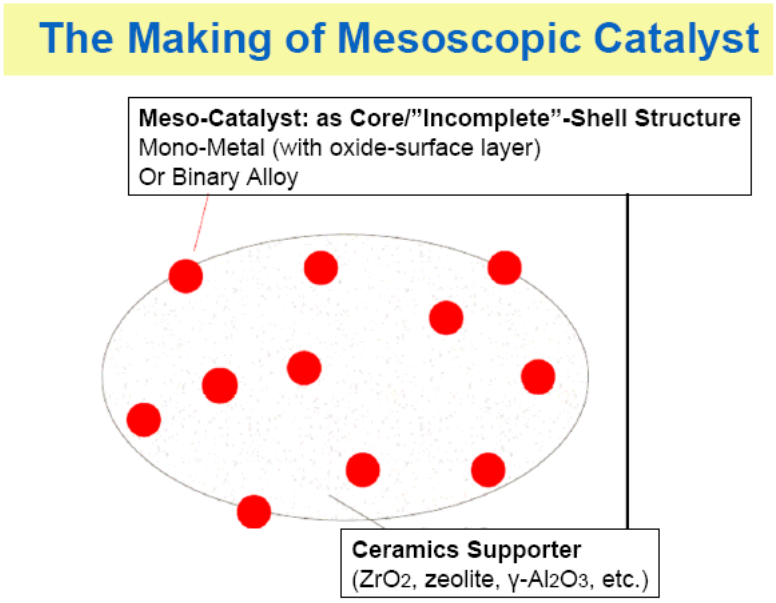

Figure 1. Design of nano-composite sample for D(H)-gas loading.

The microscopic fusion rate is defined by the time-dependent cluster condensation motion (inter-nuclear d–d distance R_{dd} and relative d–d kinetic energy) and the rate of strong interaction, using Fermi's first golden rule [4]. The D(H)-cluster formation rate should be defined to reflect, in dynamic conditions of near-surface-physics/chemistry and finite lattice of solid state physics/chemistry of condensed matter as D(H)-loaded metal electrodes, D(H)-loaded nano-metal-powder composites or some other materials used for cold fusion studies. No formulas of D(H)-cluster formation rate have been given until now, and only speculative models have been given [5,6], since the relevant dynamic conditions in condensed matter are so complex with many-particle systems. Our progress in experiments will provide hints to develop the formulas.

2. Model of TSC Formation States

We employ the idea of 'mesoscopic catalyst' [5,6] for the near-surface condition of condensed matter to provide states of dynamic TSC formation. A typical design of nano-composite metal powder in current D(H)-gas loading experiments is shown in Fig. 1. An isolated nano-binary-metal particle (1–10 nm diameter) is thought to be optimum [5,6]. It has a 'fractal' surface with many sub-nano-holes (SNH) and an inner finite lattice (Bloch) structure. The D(H)-adsorption/absorption process is illustrated in Fig. 2. An image of a TSC formation state of SNH is shown in Fig. 3. First a D_2 molecule is adsorbed at a SNH and before its dissociation the second D_2 molecule is 'orthogonally' adsorbed onto it to form a TSC ($t = 0$) state.

A diagram of absorbed D(H)s in a finite lattice of nano-particle is shown in Fig. 4 conceiving the case of Ni-core binary nano-particle at lower and higher ambient temperature.

The D_2 molecule is adsorbed and dissociated at deep trapping potential, due to many dangling chemical electron bonds there at SNH on surface. The deuterons then diffuse into inner finite lattice sites by the quantum-mechanical

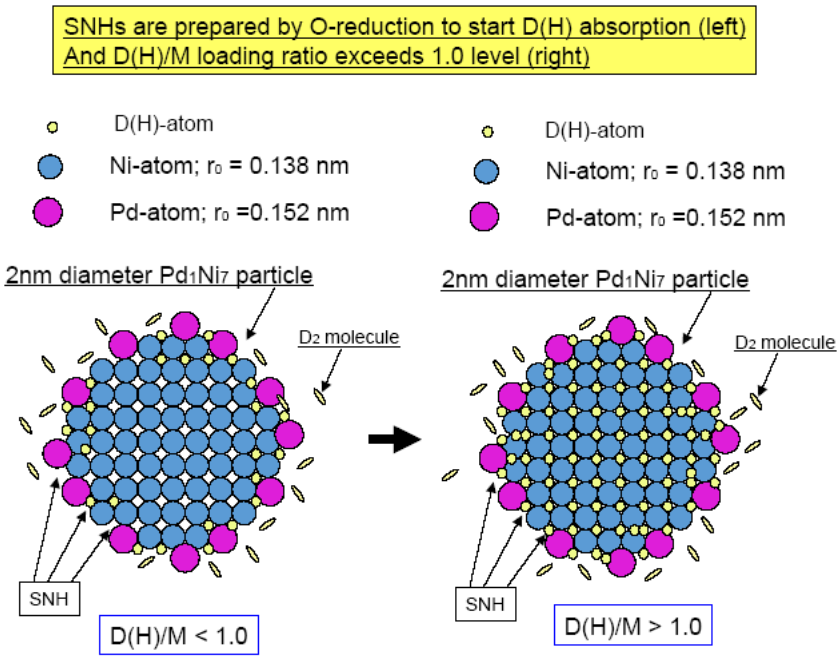

Figure 2. D(H)-adsorption/absorption image via SNHs of nano-particle.

(QM) tunneling effect, which is enhanced at elevated temperature. From the point of view of thermodynamics, system energy is transferred via phonon energy exchange between trapped D(H)s in QM oscillation and outside phonons of the substrate (a ceramic supporter) as shown in Fig. 5. The temperature dependence of phonon-frequency distribution of trapped D(H)s in GMPW (global mesoscopic potential well) should be studied.

At elevated temperature conditions, the probability of TSC ($t = 0$) formation at inner finite lattice sites may be significantly enhanced [1] as illustrated in Fig. 6. Quantitative QM calculations for these TSC formation process are very complex due to so many-body time-dependent problems under the ordering/constraint conditions of condensed matter. They will require further study.

3. Cluster Fusion Rates

Once a TSC ($t = 0$) state forms, the time-dependent TSC condensation motion is so fast, it finishes 4D/TSC condensation in 1.4 fs [2,3]. During the continuous condensation motion, we can employ an 'adiabatic' state (for digitizing very small time-steps) of 'quasi-molecule' confining potential and 4D (or d–d pair) wave function, as illustrated in Fig. 7. In the QM-Langevin calculation, Gaussian-type wave functions were employed [2,3] to implement the 'quasi-eigen-values' search for the adiabatic state, by using the variational method [3]. The detail of QM-Langevin equation and TSC-trapping potential is fully given in [2,3].

The cluster fusion rate for an adiabatic quasi-molecule state is given by Fermi's golden rule under the Born–Oppenheimer approximation.

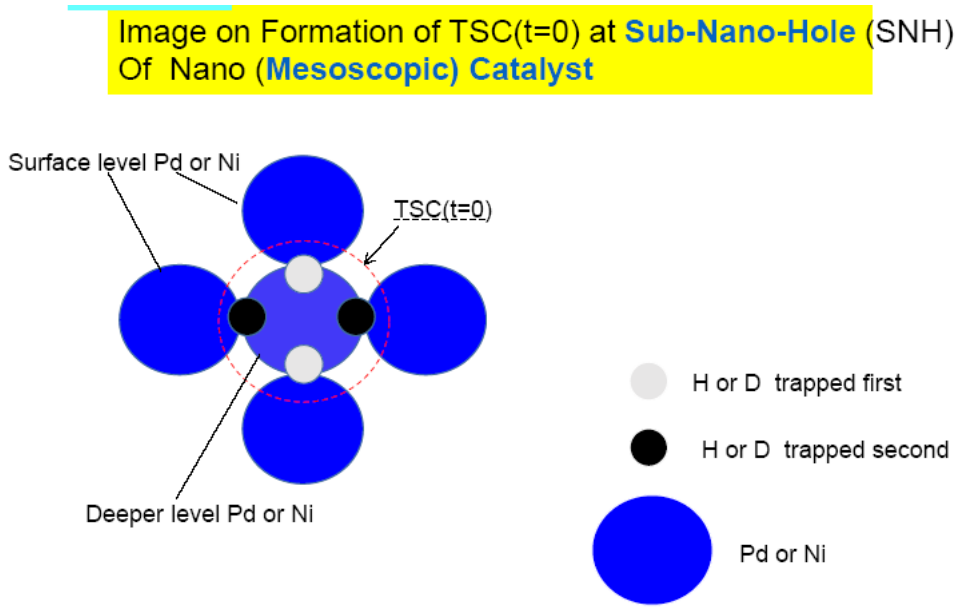

Figure 3. Image of TSC ($t = 0$) formation at a SNH state.

$$\langle \text{FusionRate} \rangle = \frac{2}{\hbar} \langle \Psi_{\text{nf}} | W(r) | \Psi_{\text{ni}} \rangle_{V_n} \cdot \langle \Psi_{\text{cf}} \mid \Psi_{\text{ci}} \rangle_{V_n} . \tag{2}$$

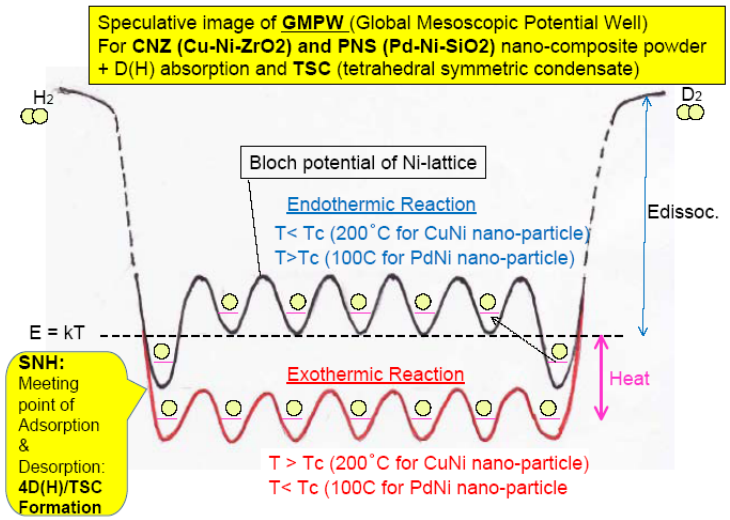

Figure 4. Diagram of absorbed D(H)s in a global mesoscopic potential well (GMPW) of binary nano-particles.

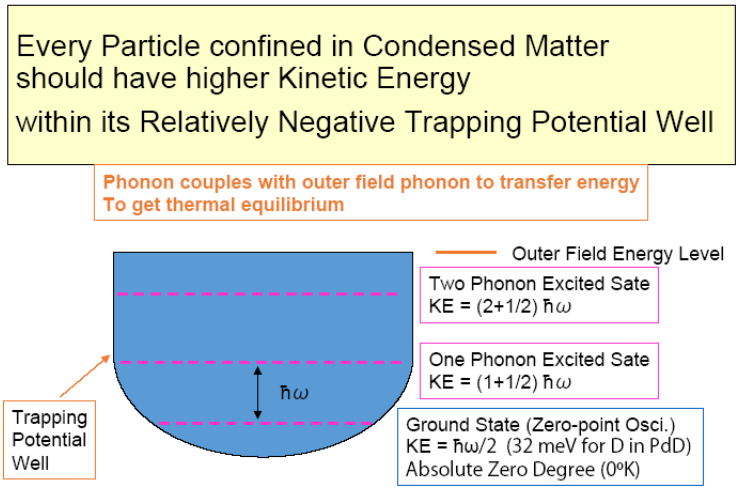

Figure 5. Phonon-energy exchange of trapped D(H)s and outer phonons in the substrate (a ceramic supporter).

Here, Ψ_{ni} and Ψ_{nf} are inter-nuclear wave functions, respectively for the initial state and the final state. Ψ_{ci} and Ψ_{cf} are outer-nuclear wave functions in the electro-magnetic field, respectively for the initial and the final state of interaction. V_n is the effective volumetric domain of nuclear interaction by strong (or weak) force to be given approximately as,

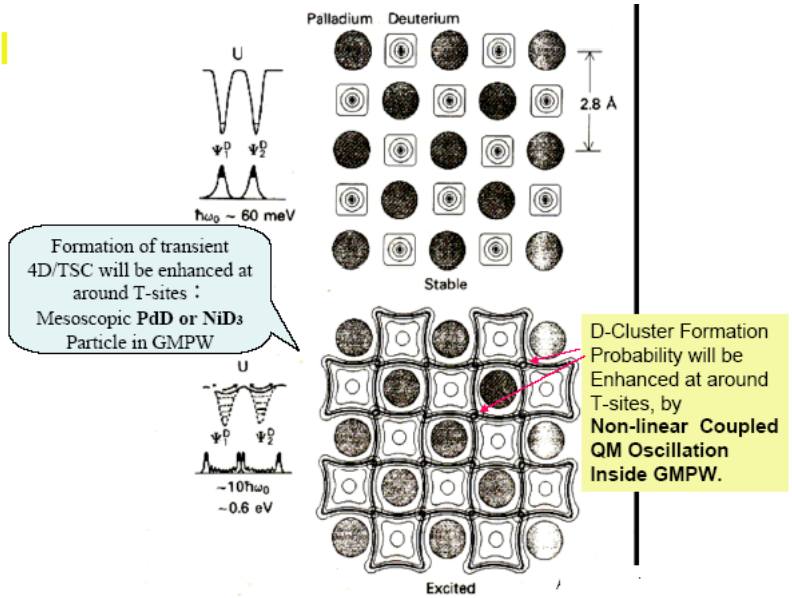

Figure 6. Possibility of enhanced TSC formation at inner lattice sites of nano-particle as mesoscopic catalyst, at elevated ambient temperature (lower figure).

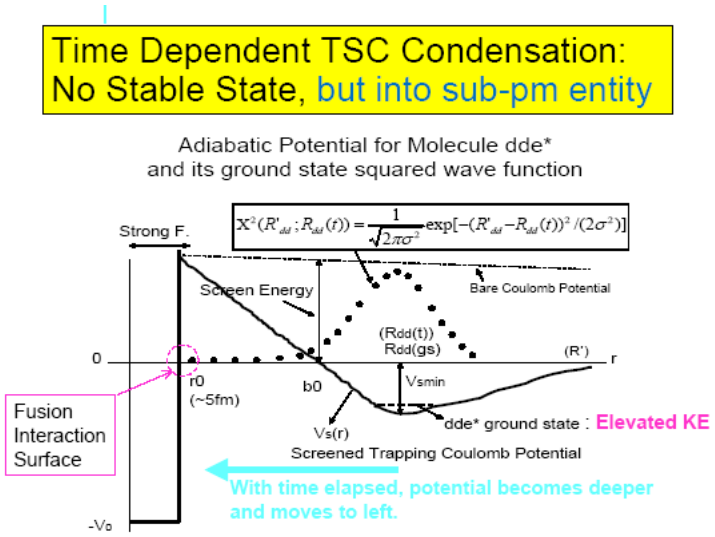

Figure 7. Illustration of 'adiabatic state' under continuous condensation motion of 4D(H)/TSC.

$$V_n \approx 4\pi R_n^2 \lambda\!\!\!^{-}_{\pi}. \tag{3}$$

Here R_n is the radius of nuclear-interaction surface as shown in Fig. 7, and $\lambda\!\!\!^{-}_{\pi}$ is the Compton wavelength (1.4 fm) of pion as virtual force-exchange boson for strong interaction. (In the case of weak interaction, we replace it with the

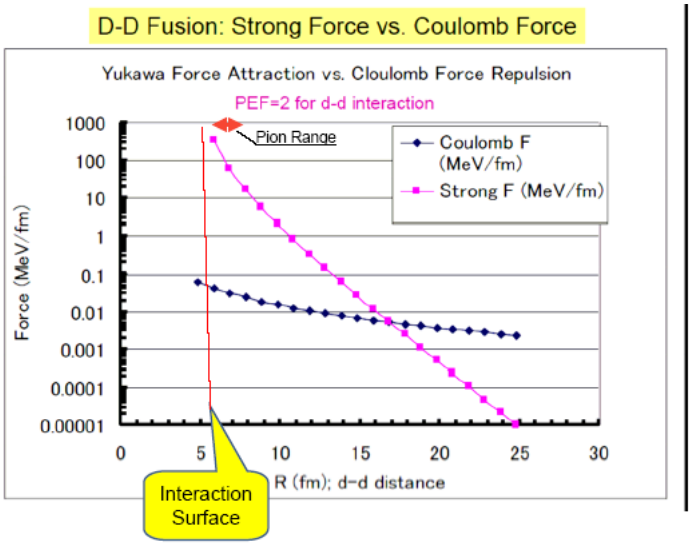

Figure 8. Strong force (attractive) is compared with Coulombic force (repulsive) for the d–d interaction.

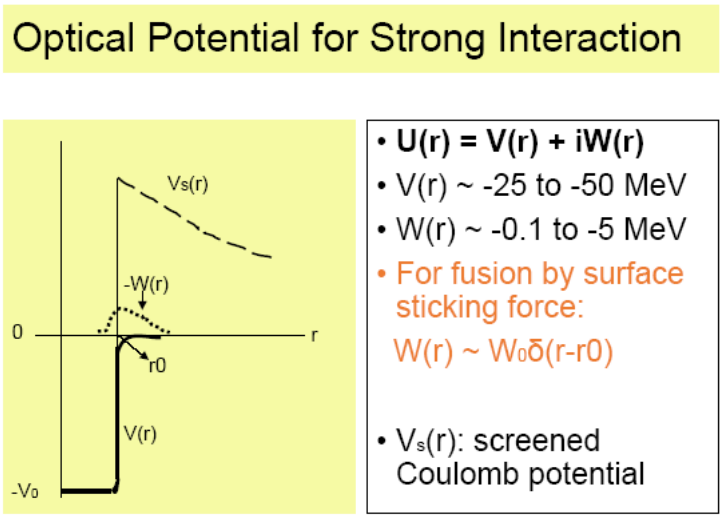

Figure 9. General features of nuclear optical potential.

Compton wavelength of weak boson 2.5 am.)

$W(r)$ is the imaginary part of the nuclear optical potential, which is the main factor of strong (or weak) interaction near around the interaction surface $r = R_n$. To estimate the fusion rate by Eq. (2), we need to calculate two adiabatic terms: the first is the inter-nuclear fusion rate, and the second is the effective QM wave-function-weight for that inter-

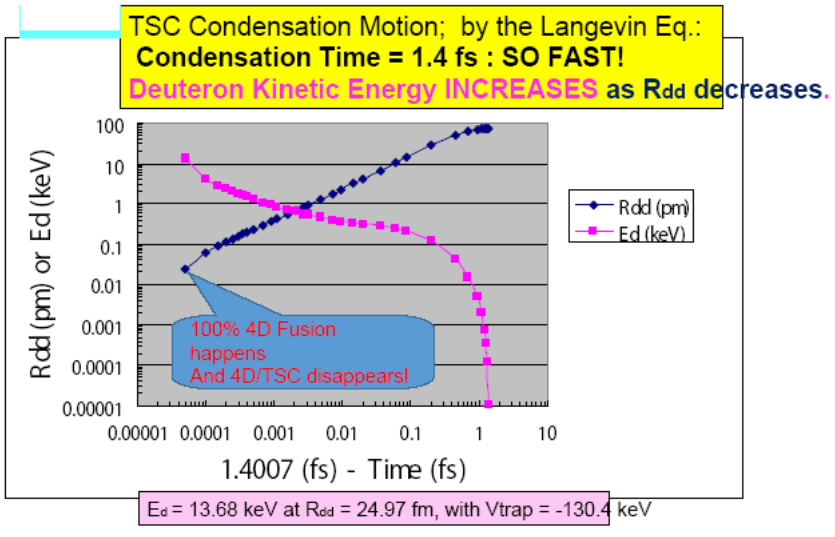

Figure 10. Time variation of R_{dd} and relative d–d kinetic energy under the 4D/TSC condensation.

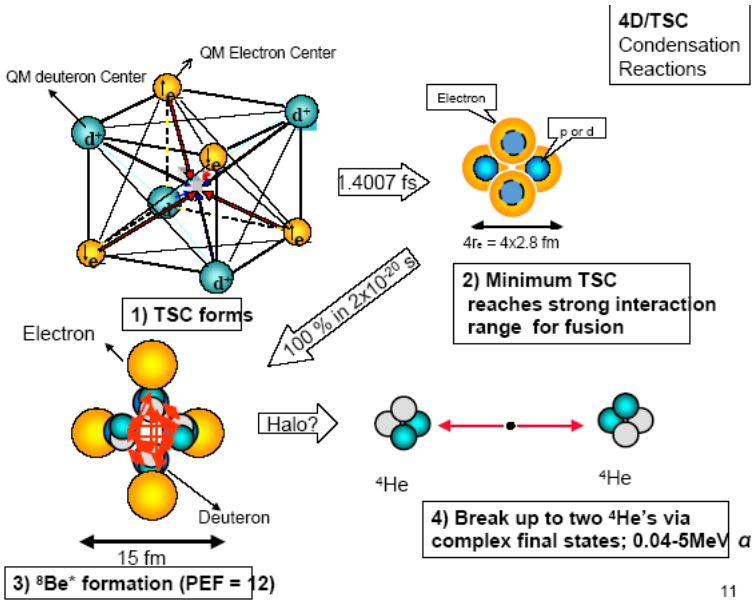

Figure 11. Brief view of 4D/TSC condensation and 4D fusion.

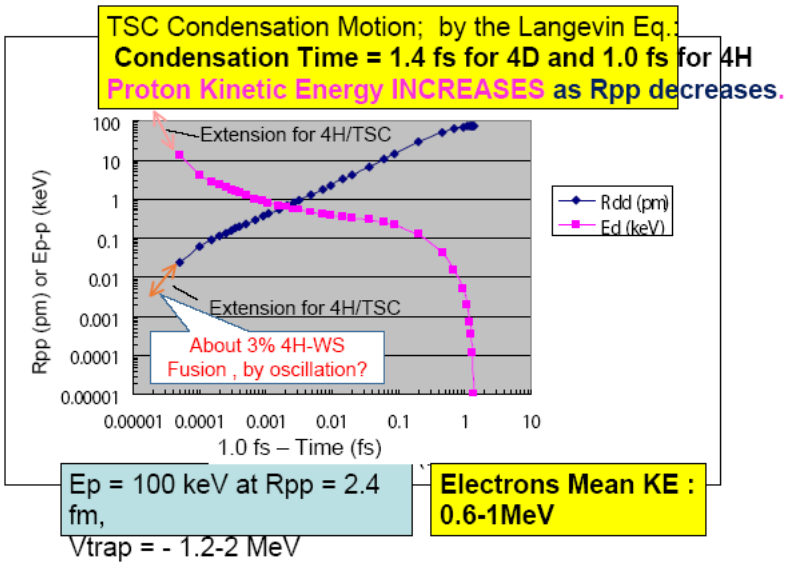

Figure 12. Time variation of R_{pp} and relative p–p kinetic energy under the 4H/TSC condensation.

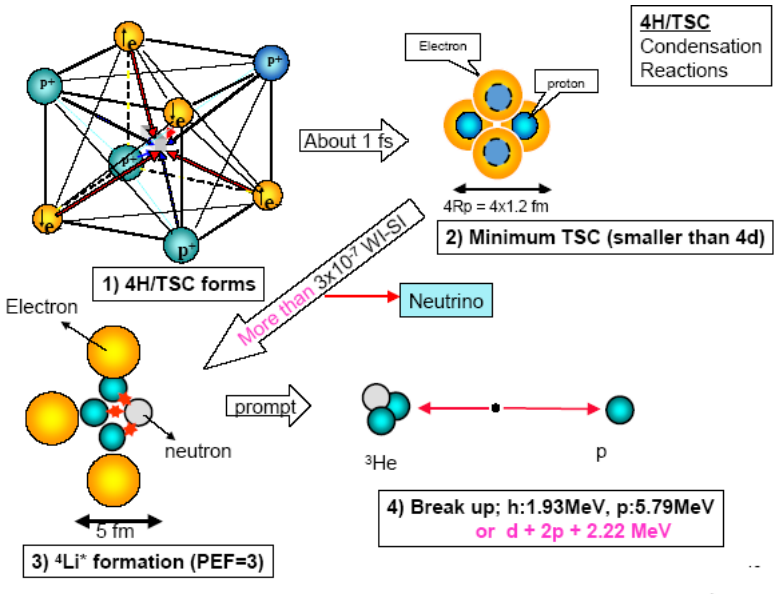

Figure 13. Brief view of 4H/TSC condensation and 4H weak-strong fusion interaction.

nuclear fusion rate [4]. In an approximate treatment, the second term is calculated by using the WKB approximation with Gamow integral, which is called the 'barrier penetration probability.' The approximation of the first term $\langle W \rangle$, an

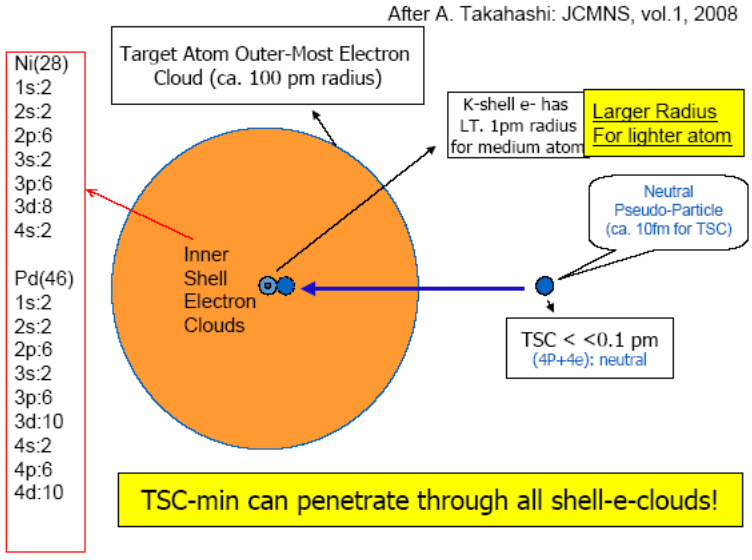

Figure 14. 4H/TSC-minimum may approach Ni-nucleus to make strong interaction (4p capture and fission).

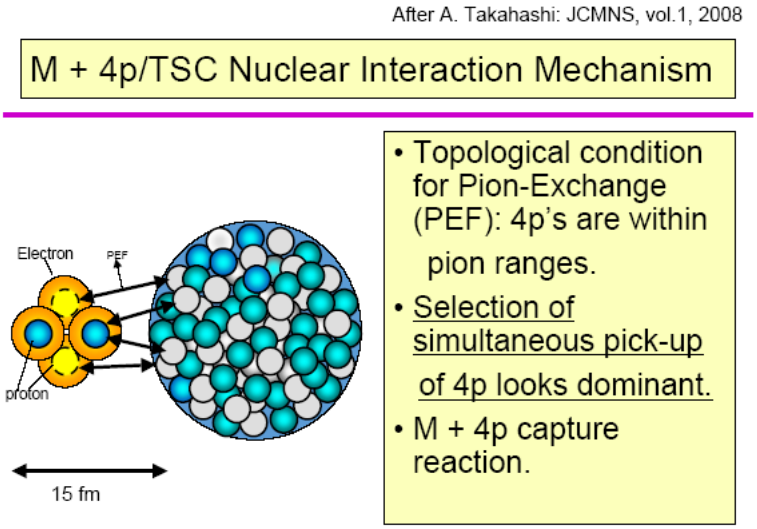

Figure 15. 4H/TSC-minimum can make 4p capture into Ni nucleus.

empirical approach with pion exchange force-values (PEF-values), was used [3,4].

A graph of PEF as a measure of strong interaction is drawn in Fig. 8 for the case of PEF =2 (d–d fusion), using

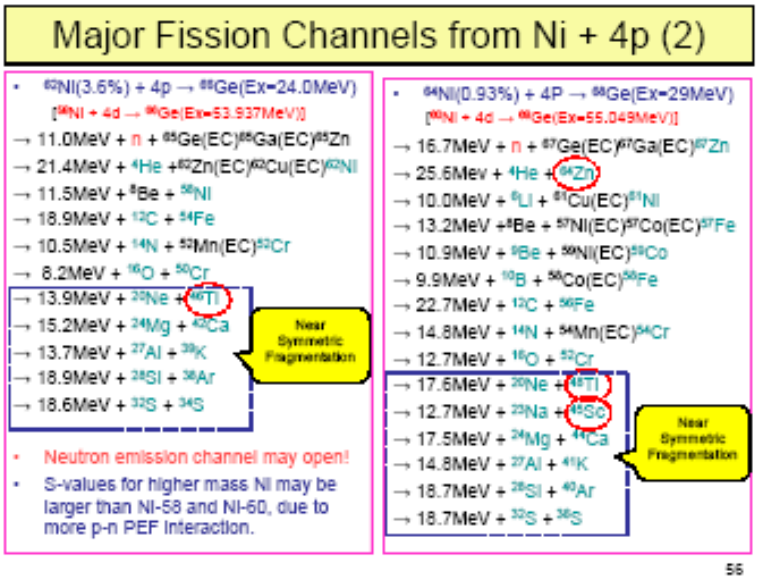

Figure 16. Expected major fission products by Ni + 4p process.

the simplified one-pion exchange potential of Hamada–Johnston [7] the main part of which is the Yukawa potential of meson exchange. $\langle W \rangle$ values for multi-bod*y*fusion as 3D, 4D and 6D were roughly estimated by using the scaling law with $(\mathrm{PEF})^5$ and cross sections of p–d, d–d and d–t reactions and were given in [3]. The general features of the nuclear optical potential is illustrated in Fig. 9.

4. D-Cluster Fusion

As soon as a 4D/TSC ($t = 0$) state with a D_2 molecule of size ($R_{dd} = 74$ pm) is formed, our code calculation by the QM-Langevin equation gives a numerical solution for time-dependent R_{dd} and mean relative kinetic energy of d–d pair of a face of six TSC (d–e–e–d-type) faces, as copied from Refs. [2,3] and shown in Fig. 10. The adiabatic size of 4D/TSC reaches few tens of femtometers in 1.4 fs, which is fast. With adiabatic 4D/TSC size around 20 fm, 4D-fusion takes place by 100% yield [2,3] in 2×10^{20} s, namely,

$$\mathrm{D} + \mathrm{D} + \mathrm{D} + \mathrm{D} \rightarrow {}^{8}\mathrm{Be}^{*}(Ex = 47.6\ \mathrm{MeV} : J^{\pi}). \tag{4}$$

The break up channels of ^{8}Be* are very complex, because break-up occurs with a very deformed nucleon (n or p) halo admixture, which may have a very small level-gap (possibly 1–10 keV) vibration/rotation band structure with relatively long life time, from where complex EM transitions to emit low energy (1–10 keV, possibly) gamma-rays and excitation-damping to the ^{8}Be ground state (two alphas decay) may occur [8]. 4D/TSC disappears after 1.4 fs.

The fusion yield per 4D/TSC generation is calculated by integrating the time-dependent fusion rate by Fermi's first golden rule as precisely explained in reference [3], that was very close to 1.0, namely 100%, during the very small time interval of ca. 2×10^{-20} s in the final stage of condensation. The mean relative kinetic energy of neighboring d-d pairs of 4D/TSC-minimum is ca. 14 keV, which by coincidence resembles the value of DT plasma fusion experimental devices such as ITER. A discussion of the mean kinetic energies of d–d pairs was given in [7] for the D_2 molecule (2.7 eV) and muonic d–d molecule (180 eV). These are not 'cold' values as 0.025 eV of room-temperature matter. The reason is that the confined d–d pair in a 'deep' electromagnetic (or Coulombic) trapping potential should decrease its de Broglie wave length to be constrained by the Heisenberg Uncertainty Principle (HUP).

A simplified image of 4D/TSC condensation and fusion reaction is copied [1–3] as shown in Fig. 11.

5. 4H/TSC WS Fusion

According to the formula of the QM-Langevin equation, the velocity of condensation (time dependent) is inversely proportional to the square root of the mass of the confined particle. Therefore, 4H/TSC will condense in 1.0 fs to the small size region of a few tens of femtometers. However, there is no strong-fusion interaction (PEF = 0) between 4 protons of TSC to finally destroy the TSC state. We believe that 4H/TSC can condense further to be ultimately as small as the 4H/TSC-minimum state, a few femtometers in size (where 2.4 fm p–p distance is the limit, due to the hard core of the proton with 1.2 fm radius). The problem there is how long the 4H/TSC-minimum state can survive.

As a future task, we need a study of this extremely condensed state using a relativistic QM equation (the Dirac equation or some equivalent one). The TSC trapping potential can be modified with an additional term of spin-tensor force of electrons and protons in combination of ordered directions [8]. The converted figure of condensation motion for 4H/TSC is shown in Fig. 12.

The depth of adiabatic p–p trapping potential on a face of TSC is as deep as –1.2 to –2.0 MeV in the 4H/TSC-minimum state. There the mean relative kinetic energy of electron E_{eke} in a p–e–e–p system on one face of TSC would be 0.6–1.0 MeV. Therefore, we may expect the electron capture process to occur with one proton of 4H/TSC-minimum, by the weak interaction [9] .

$$\mathrm{p} + \mathrm{e} + E_{eke} \rightarrow \ \mathrm{n} + \mathrm{neutrino} + E_{eke} - 272\ \mathrm{keV}. \tag{5}$$

Once a proton-to-neutron transition is generated by the electron capture, we expect instantaneous strong interaction between the newly born neutron and closely available three protons within the Compton wave length of charged pions 1.4 fm (PEF = 3) as illustrated in step (3) of Fig. 13. As the pion range 1.4 fm is the Heisenberg uuncertainty in distance, the n + 3p reaction takes place by 100% with $\langle W \rangle$ value of PEF = 3 (comparable to d–t fusion) [9].

$$3\mathrm{p} + \mathrm{n} \rightarrow {}^{4}\mathrm{Li}^{*}\ (Ex = 4.62\ \mathrm{MeV}). \tag{6}$$

The intermediate compound ^{4}Li* has two break-up channels.

$$^{4}\mathrm{Li}^{*}\ (Ex = 4.62\ \mathrm{MeV}) \rightarrow {}^{3}\mathrm{He}\ \mathrm{p} + 7.72\ \mathrm{MeV}, \tag{7}$$

$$^{4}\mathrm{Li}^{*}\ (Ex = 4.62\ \mathrm{MeV}) \rightarrow 2\mathrm{p} + \mathrm{d} + 2.22\ \mathrm{MeV}. \tag{8}$$

The branch (7) is thought to be a major out-going channel and we expect ^{3}He to be the main nuclear product.

Also 5.79 MeV proton will produce secondary neutron by Ni(n,p) reactions with higher mass nickel isotopes, on the order of 10^{-13} of ^{3}He production rate and Ni(p,γ) secondary gamma-rays on the order of 10^{-11} per 5.79 MeV proton. Characteristic X-rays from nickel ionization by the proton are also expected.

However, we do not know the branching ratio to the branch (8), which will not produce secondary neutrons and gamma-rays at all.

So the key problem is how probable is it that a weak interaction rate will suffice to generate neutron–nucleon (not a free neutron) during the duration of the 4H/TSC-minimum state. The weak interaction rate is given by

$$\langle W I \mathrm{rate} \rangle = (4\pi/h)\langle W \rangle_w \langle \Psi_e(r_w) \rangle^2 . \tag{9}$$

The details of the weak interaction rate calculation are given in [9]. As the Compton wave length of weak bosons (W^+,W^-) is extremely short, at 2.5×10^{-18} m (2.5 am), the second term of Eq. (9), namely, the weight of electron wave function from outer EM field, is as small as 5.9×10^{-5}, and the $\langle W \rangle$ value is also small, 78 eV [9].

If we assume the lifetime of 4H/TSC minimum is the same as the 4D/TSC-minimum, namely ca. 2×10^{-20} s, the weak interaction yield is very small, 3×10^{-7} fusion/TSC.

However, if the lifetime of 4H/TSC-minimum would be elongated to ca. 1 fs, which is comparable to the condensation time, the weak interaction yield can become as large as 3×10^{-2} (3%)/TSC, which is a reasonably large enough level to explain 100 W/mol-Ni–H level excess heat evolution in the Ni-based gas-loading experiments [10,11].

The other weak interaction channel is the p + p $\rightarrow$ d + β^+ + Q reaction. The p–p fusion rate at the 4H/TSC-minimum state is estimated to be 10^{-38} f/s, by using the S value 3.4×10^{-22} keV and the relative p–p kinetic energy 100 keV for the two-body reaction rate formula (Fermi's second golden rule [4]). Assuming that the lifetime is 1 fs of 4H/TSC-minimum, the p–p weak-fusion yield is 10^{-53} f/TSC, which is negligibly small.

6. Possibility of 4H/TSC + Ni Fission

As the inner-most (K) electron shell of the nickel atom has ca. 1 pm radius of 1s orbit and additional shell electrons 'protect' the nickel nucleus from an in-coming proton to make Ni + p nuclear reaction. This makes a two-body strong interaction between metal nucleus and proton (or deuteron) impossibly difficult. However, as the 4H/TSC-minimum state may have a very small size (as small as a few femtometers) and charge-neutrality, it would easily penetrate through the multi-shell barrier of electrons of metal nucleus. As nickel has a much larger 1s orbit than that of palladium, the 4H/TSC-minimum may more easily approach to the Ni-nucleus than palladium. Because the 4D/TSC disappears at sizes of a few tens of femtometers, only 4H/TSC has a good probability of approaching the nickel nucleus. This feature is illustrated in Fig. 14.

We have reported that fission products from Ni + 4p fission are predicted to be mainly clean stable isotopes, according to the selected channel scission theory [12]. As discussed in the previous section, the lifetime of the 4H/TSC-minimum state may be much longer than we conceived previously, and the size of its neutral entity is much smaller than previously thought. The strong interaction with nickel nucleus would be selective to the Ni + 4p capture and 1p to 3p capture processes will be neglected as shown in Fig. 15.

Fission products are considered to be mostly from the near symmetric fragmentations of Ge* intermediate compound state as shown in Fig. 16. In the past, there were reports on production of foreign elements, which were thought to be transmutation by several authors, such as Miley and Patterson [13].

Their data were analyzed by TSC-induced fission in reference [12]. Mass spectral analysis for samples before and after use is recommended for Ni–H system experiments as being done by the Piantelli-group, Kobe-Technova-group (Sakoh et al.) and Celani-group (INFN).

7. Conclusions

A systematic theoretical study on the possible physics mechanisms of cold fusion in D(H)-contained condensed matter is briefly explained.

As the nature of condensed matter is the ordering/constraint dynamic conditions on confining particles of deuterons, protons and electrons in electro-magnetically induced trapping potentials, D(H)-cluster formation and its transient motion is considered a clue to solve the puzzle of cold fusion.

The TSC theory has been proposed and elaborated since April 1989 by the author in three main steps [1]. The most realistic solution with quantitative results of microscopic D(H)-cluster fusion rates has been obtained recently (step 3) by using the QM-Langevin equation for studying their dynamic condensation processes and relevant strong and/or weak nuclear interactions as a many-body system. The conventional two-body system has not been able to provide meaningfully observable nuclear reaction rates, in contrast to the hot fusion process.

The 4D simultaneous fusion (^{4}He: ash) and the 4H simultaneous weak-strong fusion (^{3}He, d: ash) are the consequence of the TSC theory that the author has developed until now.

The quantitative formulation of microscopic fusion rates for D(H)-cluster fusion has been made by one-through work. However, the remaining work, namely the quantitative study on the TSC formation probability in D(H)-loaded metal systems is yet to be done. It might be accomplished by solving many-body time-dependent problems under organization of the field of condensed matter. This will be challenging.

Acknowledgment

The author is grateful to Technova colleagues (A. Kitamura, R. Seto and Y. Fujita) for their support.

References

[1] A. Takahashi, Progress in condensed cluster fusion theory, *J. Cond. Mat. Nucl. Sci.* **4** (2011) 269–281.
[2] A. Takahashi, *The Basics of Deuteron Cluster Dynamics as Shown by Langevin Equation*, American Chemical Society, Oxford Univ. Press, Oxford, LENR-NET Sourcebook, Vol.2, 2009, pp. 193–217.
[3] A. Takahashi, N. Yabuuchi, Study on 4D/TSC condensation motion by non-linear Langevin equation, American Chemical Society, Oxford Univ. Press, LENR-NET Sourcebook Vol.1, pp.57-83 (2008)
[4] A. Takahashi and N. Yabuuchi, Fusion rates of bosonized condensates, *J. Cond. Mat. Nucl. Sci.* **1** (2007) 106–128.
[5] A. Takahashi et al., Role of PdO surface coating in CMNE D(H)-gas loading experiments, *J. Cond. Mat. Nucl. Sci.* **5** (2011) 17–33.
[6] A. Takahashi et al., Mesoscopic catalyst and D-cluster fusion, *Proc. JCF11*, pp. 47–52, JCFRS web-site, (2011).

[7] A. Takahashi, Kinetic reaction energy of cold fusion, *Proc. JCF12*, Dec. 2011, Kobe, pp. 67–76 (2012).
[8] D. Rocha, Private communication with A. Takahashi, 2012.
[9] A. Takahashi, 4HTSC fusion by simultaneous weak/ and strong interactions, *Proc. JCF12*, Dec. 2011, Kobe, pp.115–122 (2012).
[10] F. Piantelli et al., Some results from the Nichenergy laboratory, presentation at the 10th Int. Workshop, Siena, April 2012 (see ISCMNS web site).
[11] H. Sakoh et al., Hydrogen isotope absorption and heat release characteristics of a Ni-based sample, *Proc. ICCF17*, Daejeon Korea, August 2012,, to be published.
[12] A. Takahashi, TSC-induced nuclear reactions and cold transmutations, *J. Cond. Mat. Nucl. Sci.* **1** (2007) 86–96.
[13] G. Miley and J. Patterson, *J. New Energy* **1** (1996) 5.